Published in final edited form as:
Cell Metab. 2014 July 1; 20(1): 133–144. doi:10.1016/j.cmet.2014.05.001.

Liver Damage, Inflammation and Enhanced Tumorigenesis after Persistent mTORC1 Inhibition

Atsushi Umemura[1], **Eek Joong Park**[3], **Koji Taniguchi**[1], **Jun Hee Lee**[4], **Shabnam Shalapour**[1], **Mark A. Valasek**[2], **Mariam Aghajan**[1], **Hayato Nakagawa**[1,5], **Ekihiro Seki**[3], **Michael N. Hall**[6], and **Michael Karin**[1,7]

[1]Laboratory of Gene Regulation and Signal Transduction, Departments of Pharmacology, University of California San Diego, 9500 Gilman Drive, La Jolla, San Diego, CA 92093, USA [2]Pathology, Moores Cancer Center, University of California San Diego, 9500 Gilman Drive, La Jolla, San Diego, CA 92093, USA [3]Department of Medicine, School of Medicine, University of California San Diego, 9500 Gilman Drive, La Jolla, San Diego, CA 92093, USA [4]Department of Molecular and Integrative Physiology, University of Michigan Geriatrics Center, 109 Zina Pitcher Place, 3019 BSRB, Ann Arbor, MI 48109-2200, USA [5]Department of Gastroenterology, Graduate School of Medicine, University of Tokyo, 7-3-1 Hongo, Bunkyo-ku, Tokyo 113-8655, Japan [6]Biozentrum, University of Basel, Klingelbergstrasse 70, CH4056 Basel, Switzerland

Summary

Obesity can result in insulin resistance, hepatosteatosis and non-alcoholic steatohepatitis (NASH) and increases liver cancer risk. Obesity-induced insulin resistance depends, in part, on chronic activation of mammalian target of rapamycin complex 1 (mTORC1), which also occurs in human and mouse hepatocellular carcinoma (HCC), a frequently fatal liver cancer. Correspondingly, mTORC1 inhibitors have been considered as potential NASH and HCC treatments. Using a mouse model in which high fat diet enhances HCC induction by the hepatic carcinogen DEN we examined whether mTORC1 inhibition attenuates liver inflammation and tumorigenesis. Notably, rapamycin treatment or hepatocyte-specific ablation of the specific mTORC1 subunit Raptor resulted in elevated interleukin 6 (IL-6) production, activation of STAT3 and enhanced HCC development, despite a transient reduction in hepatosteatosis. These results suggest that long term rapamycin treatment, which also increases IL-6 production in humans, is unsuitable for prevention or treatment of obesity-promoted liver cancer.

[7]To whom correspondence should be addressed at karinoffice@ucsd.edu.

Introduction

Rapamycin is a macrolide produced by the bacterium *Streptomyces hygroscopicus* found in a soil sample from Easter Island (Vezina et al., 1975). Also known as sirolimus, rapamycin was originally developed as an antifungal agent, but soon its potent immunosuppressive activity was discovered and studied before its mechanism of action was fully understood, resulting in FDA approval in 1999 for post-kidney transplantation therapy. The chief advantage of rapamycin over calcineurin inhibitors is reduced kidney toxicity. Since then, rapamycin and several derivatives, including everolimus and temsirolimus, collectively referred to as 'rapalogs', were approved for a variety of indications (Benjamin et al., 2011; Johnson et al., 2013). The target for these drugs is the large (289 kDa) protein kinase Target of Rapamycin (TOR) (Heitman et al., 1991), in mammals known as mTOR, which forms two functionally distinct multi-protein complexes, mTOR complex 1 (mTORC1) and mTOR complex 2 (mTORC2) (Wullschleger et al., 2006). mTORC1, composed of mTOR, raptor and mLST8, is a master regulator of cellular growth and metabolism that is activated by nutrients and growth factors. Most of the effects of rapamycin are due to inhibition of mTORC1 (Wullschleger et al., 2006). Accordingly, rapalogs are potent suppressors of cellular proliferation and growth and can revert several metabolic disorders, such as insulin resistance and hepatosteatosis, caused by persistent mTORC1 activation after hypernutrition (Cornu et al., 2013; Duvel et al., 2010).

Because mTORC1 is activated in well in over 50% of human cancers (Menon and Manning, 2008; Shaw and Cantley, 2006), there has been much interest in using rapalogs in cancer treatment (Abraham and Gibbons, 2007; Guertin and Sabatini, 2007; Sabatini, 2006). The mTOR pathway is also upregulated in up to 50% of hepatocellular carcinomas (HCCs), the major form of liver cancer, and PTEN, the tumor suppressor that inhibits mTORC1 activation, is inactivated in many such tumors (Bhat et al., 2013; Hu et al., 2003). Moreover, obesity, hepatosteatosis and insulin resistance, pathologies precipitated by hypernutrition and chronic mTORC1 activation, are associated with a pronounced increase in HCC risk (Calle et al., 2003). In fact, obesity is quickly becoming a major driver of HCC, which together with NASH, is one of the most serious complications of hypernutrition. Given the likely involvement of mTORC1 in hepatosteatosis and cancer it was suggested that rapalogs may be useful in HCC prevention and treatment (Bhat et al., 2013; Faloppi et al., 2011). However, rapalogs had limited success as single-agent cancer therapies in hundreds of clinical trials to date, and their activities in most cancer types have been modest at best (Abraham and Gibbons, 2007; Chiang and Abraham, 2007; LoPiccolo et al., 2008). Clinical trials using rapalogs in HCC were also disappointing; in a phase I/II study of everolimus, only one out of 28 HCC patients had a partial response (Zhu et al., 2011). Very recently, a global phase III study showed that everolimus did not extend overall survival compared to placebo in patients with locally advanced or metastatic HCC after progression on or sorafenib intolerance (ClinicalTrials.gov Identifier: NCT01035229) (Health., 2013; Novaritis, 2013). In addition, everolimus use for HCC treatment was found to result in increased incidence of liver injury (Yamanaka et al., 2013; Zhu et al., 2011).

These unexpected outcomes may be due to a poor understanding of the role of mTORC1 and the effect of its inhibition in liver pathophysiology and tumorigenesis. In terms of liver

transplantation, NASH is now the third most common indication in the US, and is the only indication consistently increasing in frequency along with the alarming prevalence of the metabolic syndrome and its associated complications among liver transplant recipients. If current trends continue, NASH will become the most common indication for liver transplantation in the US within 10-20 years. Thus, it is particularly important to determine the impact of rapalogs on hepatosteatosis, NASH and other conditions associated with the metabolic syndrome (Watt, 2012). Curiously, despite its beneficial effects in kidney transplantation, sirolimus is not recommended for use after liver transplantation because of excess mortality, graft loss, and hepatic artery thrombosis (HAT) (Massoud and Wiesner, 2012). Although everolimus was approved in February 2013 for liver transplantation, there seems to be a concern about its use for this indication according to a recent clinical study that reported 13/245 (5.3%) deaths in the everolimus group compared to 7/243 (2.9%) deaths in the control group during the first 12 months of use [Full prescribing information of ZORTRESS (everolimus); Reference ID: 3262062]. Most deaths were associated with liver-related issues, infections and sepsis. Furthermore, the incidence of hepatitis in old mice receiving long term rapamycin treatment was increased compared to controls, although it was not significant because of a small sample size (Neff et al., 2013). Such results stand in marked contrast to reports of rapamycin-induced life-span extension (Harrison et al., 2009; Johnson et al., 2013), although follow up studies discovered several adverse effects of long term rapamycin use (Lamming et al., 2012; Neff et al., 2013).

In the present study, we used rapamycin treatment and liver-specific raptor deficient mice to determine the effect of systemic and cell type-specific mTORC1 suppression on liver physiology and tumorigenesis. Although rapamycin reduced hepatosteatosis, it increased IL-6 production and activated the pro-tumorigenic factor STAT3, resembling effects that were observed in human patients (Buron et al., 2013). Furthermore, hepatocyte-specific loss of mTORC1 activity resulted in low grade liver damage and inflammation and a marked enhancement of hepatocarcinogenesis. These results suggest that long term mTORC1 inhibition may not be a valid therapeutic option in NASH or steatotic HCC.

Results

Rapamycin reduces hepatosteatosis but increases IL-6 and STAT3

To examine whether mTORC1 inhibition reverses hepatosteatosis caused by high fat diet (HFD) and thereby can reduce HCC risk, we placed male BL6 mice on normal chow or HFD for 3 months and then treated them with rapamycin while maintaining the same feeding regimens. As expected, mice on HFD exhibited marked hepatosteatosis, but two weeks of rapamycin treatment decreased liver lipid droplets and reactive oxygen species (ROS) content (Figures 1A, B). However, as previously observed in humans (Buron et al., 2013) and mice (Weichhart et al., 2008), rapamycin treatment enhanced liver damage due to HFD feeding and increased IL-6 production, resulting in activation of the oncogenic transcription factor STAT3 in liver tissue (Figures 1C, D). Rapamycin treatment reduced accumulation of the autophagy substrate p62 and increased the LC3 II:I ratio (Figure S1A) and decreased the mRNA expression of the lipogenic transcription factor SREBP1c, but it also decreased expression of the anti-inflammatory cytokine IL-10 (Figure S1B). Thus,

while enhancing autophagy, a beneficial effect, rapamycin treatment also had adverse pro-inflammatory effects. To determine whether strong mTORC1 inhibition leads to hepatocyte death, we incubated a normal hepatocyte cell line, AML12, with 10-100 μM rapamycin. As found in other cell types (Galluzzi et al., 2012; Yellen et al., 2011), 16 hrs of incubation with 10-100 μM of rapamycin resulted in considerable cell death and caspase activation (Figure S1C-E).

Liver specific Raptor knockout mice

Some of the adverse effects observed in vivo could be due to mTORC1 inhibition in cells other than hepatocytes, such as macrophages (Mercalli et al., 2013; Weichhart et al., 2008). To examine whether long term mTORC1 inhibition only in liver parenchymal cells circumvents these effects, we generated hepatocyte-specific raptor-deficient mice (*Raptor*$^{\Delta hep}$) by crossing *Raptor*$^{F/F}$ mice (Bentzinger et al., 2008) with Alb-Cre mice. Deletion of the *Raptor*^{F} allele was confirmed by PCR of genomic DNA from isolated hepatocytes, although whole liver tissue of *Raptor*$^{\Delta hep}$ mice retained some of the “floxed” allele due to presence of non-parenchymal cells (Figure 2A). Immunoblot analysis of *Raptor*$^{\Delta hep}$ liver revealed a strong reduction in raptor protein (Figure 4F) and its complete absence in isolated hepatocytes (Figure 2A). The amount of phospho-p70S6K (p-S6K), a major mTORC1 substrate, was greatly reduced in *Raptor*$^{\Delta hep}$ livers (Figure 4F) and almost completely absent in isolated hepatocytes (Figure 2A). The amount of phospho-Ser473-PKB/AKT (p-AKT) and its downstream targets, phospho-Ser21 and phospho-Ser9-GSK3 (p-GSK3) were strongly elevated in *Raptor*$^{\Delta hep}$ livers (Figure 4F), indicating inhibition of mTORC1 activity and hyperactivation of AKT due to loss of a negative feedback loop (Bentzinger et al., 2008; Cornu et al., 2013). *Raptor*$^{\Delta hep}$ mice were obtained at the expected frequency and appeared healthy after birth. Yet, at 2 months of age they showed signs of liver injury (Figure 2B) and hepatocyte abnormalities, such as large cells with enlarged and hyperchromatic nuclei (Figures 2C and S2A). In addition, mild fibrotic changes (Figures 2C, S2B, and S2C), immune cell infiltration (Figures 2C, D), hepatocyte cell death, and p-γH2AX positive hepatocytes which implicate DNA damage or stalled DNA replication forks (Figures 2E, F) were increased in *Raptor*$^{\Delta hep}$ livers. Although Ki67- and p-ERK-positive cells were not increased, cyclin D1-positive cells were markedly elevated in *Raptor*$^{\Delta hep}$ livers (Figure S2D).

Loss of Raptor impairs hepatocyte proliferation and mitosis

mTORC1 was reported to regulate cell cycle and liver regeneration (Espeillac et al., 2011), promoting G2/M transition and mitosis (Gwinn et al., 2010; Nakashima et al., 2008; Ramirez-Valle et al., 2010). To investigate hepatocyte proliferation, two-thirds partial hepatectomy (PH) was performed on 8 weeks old mice. *Raptor*$^{\Delta hep}$ mice exhibited higher serum ALT (Figure 3A) and marked cytoplasmic clearing of hepatocytes, indicating hepatocytic damage and aberrant regeneration with glycogen accumulation as confirmed by PAS and PAS diastase (PASD) staining (Figures 3B, S3A, and S3B). Although liver / body weight ratio of *Raptor*$^{\Delta hep}$ mice appeared to be reduced 48 hrs after PH, the effect was not significant (Figures 3A).

Bromodeoxyuridine (BrdU)-incorporating and Ki67-positive hepatocytes were reduced, but cyclin D1 positive cells were increased after PH in *Raptor*$^{\Delta hep}$ mice compared with *Raptor*$^{F/F}$ mice (Figure 3C). Since H&E staining revealed fewer mitotic figures in *Raptor*$^{\Delta hep}$ than *Raptor*$^{F/F}$ livers (Figures 3B and S3A), mitosis was also examined using the mitotic markers phospho-Histone H3 and cyclin B (Gwinn et al., 2010; Merlen et al., 2013) (Figure 3D). The frequency of mitosis after PH was drastically reduced in *Raptor*$^{\Delta hep}$ livers, along with cyclin B, cyclin E, cdc2, p21, and p27 and elevation of cyclin D1 (Figure 3E). In addition to p-AKT and p-GSK3, phosphorylated (activated) ERK (p-ERK) and STAT3 (p-STAT3) were also elevated in *Raptor*$^{\Delta hep}$ livers (Figure 3E). Taken together, raptor ablation interferes with hepatocyte proliferation impacting mainly G2/M transition and mitosis. However, liver regeneration was not impaired and all *Raptor*$^{\Delta hep}$ mice survived PH, because hepatocyte overgrowth due to persistent activation of AKT, ERK, and STAT3 and overexpression of cyclin D1 may have compensated for defective mitosis. Nonetheless, the raptor deficiency results in damage to the regenerating liver.

Loss of Raptor augments hepatocellular death and inflammation

In addition to being a carcinogen, diethylnitrosamine (DEN) triggers DNA damage, cell death responses and compensatory proliferation in the liver (Maeda et al., 2005). We injected 8 weeks old *Raptor*$^{F/F}$ and *Raptor*$^{\Delta hep}$ males with 100 mg/kg DEN to evaluate the impact of persistent mTORC1 inhibition on these responses. *Raptor*$^{\Delta hep}$ mice exhibited a more substantial increase in serum ALT after DEN challenge than *Raptor*$^{F/F}$ mice (Figure 4A). Cytoplasmic clearing, indicative of hepatocytic damage and aberrant regeneration with glycogen accumulation, was much more substantial in DEN-challenged *Raptor*$^{\Delta hep}$ mice than in *Raptor*$^{F/F}$ mice (Figures 4B and S4D). Correspondingly, DEN-challenged *Raptor*$^{\Delta hep}$ mice exhibited higher expression of cyclin D1 (Figures 4F and S4C), higher serum IL-6 (Figure S4A) and increased ROS accumulation (Figure S4B) compared to *Raptor*$^{F/F}$ mice. Thus, whereas short term rapamycin treatment of obese mice reduces ROS accumulation in the liver, long term mTORC1 inhibition enhances liver damage and oxidative stress in the DEN-challenged liver. Indeed, some ROS accumulation in the raptor deficient liver was seen even prior to DEN challenge (Figure S4B). The numbers of Ki67 and phospho-ERK positive hepatocytes were similar, but more cyclin D1 positive hepatocytes were found in DEN-challenged *Raptor*$^{\Delta hep}$ livers (Figure 4C). TUNEL and cleaved-caspase 3 staining revealed increased hepatocyte death in DEN-challenged *Raptor*$^{\Delta hep}$ mice (Figure 4D). Immunostaining for F4/80, B220, and CD3 indicated greater accumulation of macrophages, B and T lymphocytes after DEN administration in *Raptor*$^{\Delta hep}$ than in *Raptor*$^{F/F}$ livers (Figure 4E). Immunoblotting showed more p-STAT3, p-Akt, p-GSK3 and cyclinD1 but less p27 in DEN-challenged *Raptor*$^{\Delta hep}$ livers (Figure 4F). Expression of mRNAs for IL-6, TNF, TGFβ, IL-1β, immune cell markers and the cell death mediators DR5, TRB3, TRAIL and Bim were also elevated in the raptor-deficient liver (Figure S4C). Thus, *Raptor* ablation potentiated DEN-induced liver damage and hepatocyte death.

Loss of mTORC1 activity enhances hepatocarcinogenesis

To determine the role of mTORC1 in hepatocarcinogenesis, 14 days old male *Raptor*$^{F/F}$ and *Raptor*$^{\Delta hep}$ mice were injected with 25 mg/kg DEN (Maeda et al., 2005). At 7 months of

age, untreated mice revealed no spontaneous tumors, while all mice given DEN developed typical HCCs (Figure 5A). Strikingly, the number of detectable tumors was approximately seven-fold higher in *Raptor*$^{\Delta hep}$ mice than in *Raptor*$^{F/F}$ mice, and maximal tumor sizes were also higher (Figure 5B). Raptor expression was markedly reduced in both the non-tumor and tumor portions of *Raptor*$^{\Delta hep}$ livers (Figure 5C) and the tumors all contained the deleted *Raptor* allele (Figure S5). To further characterize the HCCs in *Raptor*$^{\Delta hep}$ mice, we cultured isolated HCC cells for several weeks as described (He et al., 2010). *Raptor*$^{\Delta hep}$ HCC cells exhibited almost complete loss of raptor and p-p70S6K and increased p-AKT and enhanced proliferation relative to dih10 cells, which were established from *WT* HCC (Figures S5B, C). Treatment of *Raptor*$^{\Delta hep}$ and dih10 HCC cells with the AKT inhibitor MK2206 resulted in inhibition of AKT phosphorylation (Figure S5B). In the raptor-deficient HCC cells the AKT inhibitor also led to enhanced caspase3 cleavage and reduced cell viability (Figures S5B, C). These results suggest that hyperactivation of AKT contributes to enhanced HCC development in *Raptor*$^{\Delta hep}$ livers. Importantly, the number and maximal size of DEN-induced HCCs in *Raptor*$^{\Delta hep}$ mice kept on high fat diet (HFD) tended to be higher than in LFD-fed *Raptor*$^{\Delta hep}$ mice or HFD-fed *Raptor*$^{F/F}$ mice (Figures 5A, B). Thus, contrary to our initial expectations, suppression of mTORC1 activity does not interfere with, and actually enhances, obesity-promoted HCC development.

Raptor deficiency augments liver fibrosis and does not improve metabolic parameters in obese mice

We analyzed 7 months old HFD-fed *Raptor*$^{\Delta hep}$ and *Raptor*$^{F/F}$ mice to evaluate the impact of mTORC1 inhibition on obesity-induced liver pathophysiology. Serum ALT was higher in HFD-fed *Raptor*$^{\Delta hep}$ mice than in *Raptor*$^{F/F}$ mice (Figure S6A). Although hepatosteatosis and hepatic TG content were similar in both groups, the degree of fibrosis in HFD-fed *Raptor*$^{\Delta hep}$ mice was significantly higher than in *Raptor*$^{F/F}$ mice (Figures 6A-C). Glucose tolerance test revealed that raptor ablation improved glucose tolerance only in LFD-fed mice, but not in HFD-fed mice (Figure 6D). We also evaluated reduced glutathione (GSH), oxidized glutathione (GSSG), and GSH/GSSG ratio. Both GSH and the GSH/GSSG ratio were significantly lower and GSSG was higher in HFD- and LFD-fed *Raptor*$^{\Delta hep}$ livers than in *Raptor*$^{F/F}$ livers (Figure S6B).

Discussion

Rapamycin is a potent anti-proliferative agent that reverses many adverse effects associated with chronic mTORC1 activation. Given frequent mTORC1 activation in cancer, including 50% of HCCs (Bhat et al., 2013), there has been much interest in the use of rapamycin and rapalogs as anti-cancer drugs (Cornu et al., 2013; Guertin and Sabatini, 2007; Menon and Manning, 2008; Shaw and Cantley, 2006). This interest has been particularly high in HCC, because in addition to genetic loss of negative regulators that function as tumor suppressors, mTORC1 is activated in response to obesity which greatly enhances HCC risk in men (Calle et al., 2003) and mice (Park et al., 2010). Consequently, we observed that obesity-promoted HCC induction in mice was accompanied by strong mTORC1 activation and postulated that together with low grade inflammation, mTORC1 activation contributes to enhanced hepatocarcinogenesis in obese mice (Park et al., 2010). We attempted to test this hypothesis

by checking whether rapamycin attenuates obesity-promoted mTORC1 activation and consequent HCC development. However, we were surprised to find that even short term rapamycin treatment resulted in increased IL-6 production and activation within liver tissue of transcription factor STAT3, previously shown to enhance HCC development (He et al., 2013). In the course of these studies we became aware of reports that rapamycin enhances IL-6 and TNF and reduces IL-10 expression both in isolated macrophages (Mercalli et al., 2013; Weichhart et al., 2008) and in human (Buron et al., 2013). To determine whether these pro-inflammatory effects are solely due to mTORC1 inhibition in macrophages, we generated hepatocyte-specific raptor-deficient mice. Although hepatocyte-specific mTORC1 activation brought about by *Tsc1* ablation results in spontaneous HCC development (Menon et al., 2012), a finding we have confirmed (unpublished results), complete mTORC1 inhibition did not attenuate DEN-induced HCC development in the absence or presence of dietary obesity. On the contrary, hepatocyte-specific raptor ablation strongly potentiated HCC induction in lean and obese mice. Thus, mTORC1 activation is unlikely to contribute to obesity-promoted HCC development, at least in this model. Most likely the cause of enhanced hepatocarcinogenesis in $Raptor^{\Delta hep}$ mice is the modest but persistent increase in liver damage and fibrogenesis. Although modest, this liver damage leads to low grade inflammation manifested by elevated macrophage infiltration into the $Raptor^{\Delta hep}$ liver. Furthermore, liver damage in $Raptor^{\Delta hep}$ mice is enhanced after PH or DEN administration. Although its exact cause is not entirely clear, liver damage in $Raptor^{\Delta hep}$ mice is likely to be due to the absence of the protective function of mTORC1 required for enhanced protein synthesis, as well as defective mitosis. Activation of AKT may further augment liver damage and tumorigenesis. Notably, previous studies also revealed tissue damage, fibrosis and inflammation upon muscle-specific raptor ablation and these effects were not relieved by additional mTORC2 inactivation, which did not prevent AKT hyperactivation (Bentzinger et al., 2008). Curiously, sustained mTORC1 activation in muscle brought about by *Tsc1* ablation also resulted in myopathy (Castets et al., 2013), resembling what was found in the liver (Menon et al., 2012). In conclusion, in addition to enhanced production of inflammatory cytokines and decreased expression of IL-10, the adverse effects of long term mTORC1 inhibition include elevated liver damage, and oxidative stress. Aberrant liver regeneration, also seen after rapamycin or temsirolimus treatment (Espeillac et al., 2011) and in $Raptor^{\Delta hep}$ livers, is another reason to be concerned about long term rapalog use, because live-donor liver transplantation, which requires regeneration, is a major treatment option for advanced NASH and localized HCC.

Although rapamycin prevents spontaneous liver damage, fibrosis and tumorigenesis in hepatocyte-specific *Tsc1* knockout mice (Menon et al., 2012), in normal mice, even those that are kept on HFD, the adverse effects of mTORC1 inhibition outweigh its benefits. Although temporary mTORC1 inhibition reduced hepatosteatosis in HFD-fed mice, after 7 months of hepatocyte specific raptor ablation obesity-driven hepatosteatosis and glucose intolerance were not ameliorated. These effects are comparable to clinical findings according to which 60% of patients receiving rapalogs require lipid lowering therapy and are at a higher risk for post-transplant diabetes (Barlow et al., 2013; Peddi et al., 2013). Recently, increased liver damage was also observed during clinical testing of an active site second generation mTOR inhibitor (Matter et al., 2013). Since some of the adverse effects of

mTORC1 activation may be due to hyperactivation of AKT and inhibition of autophagy, other approaches for inhibiting AKT activity and enhancing autophagic clearance of lipid droplets (Singh et al., 2009) may be more suitable for reducing the risk of obesity-promoted NASH and HCC development, a rapidly growing public health problem.

Experimental Procedures

Animals and liver analysis

Raptor$^{F/F}$ mice were generated as described (Bentzinger et al., 2008) and backcrossed to C57BL/6 mice at least 7 generations and bred with *Alb-Cre* transgenic mice to generate *Raptor*$^{F/F}$; *Alb-Cre* (*Raptor*$^{\Delta hep}$) mice. Genotyping was performed as described previously (Bentzinger et al., 2008).

All animal studies were performed in accordance with NIH guidelines for use and care of live animals and were approved by University of California, San Diego (UCSD) Institutional Animal Care and Use Committee, S00218. All mice were maintained in filter-topped cages on autoclaved chow diet (low-fat diet; LFD, composed of 12% fat, 23% protein, 65% carbohydrates based on caloric content) or high-fat diet (HFD, composed of 59% fat, 15% protein, 26% carbohydrates based on caloric content; BioServ) and water at UCSD according to NIH Guidlines.

In the DEN-induced HCC model, DEN (25 mg/kg) was injected intraperitoneally (i.p.) into 14 days old male mice. After 4 weeks, mice were separated into two dietary groups and fed either LFD or HFD until sacrificed at 7 months of age. In the DEN-induced acute liver injury model, DEN (100 mg/kg) was i.p. injected into 8 week-old mice.

All mice were sacrificed and their livers were removed and separated into individual lobes. Externally visible tumors (>1 mm) were counted and measured. Large lobes were fixed in 10% formalin for 24-48 hrs or embedded in Tissue-Tek OCT compound (Sakura Finetek) for paraffin or frozen block preparation, respectively. Frozen tissue sections were stained with oil-red O (ORO) for lipid, dihydroethidine (DHE) for ROS, and anti-smooth muscle actin (SMA) antibody (abcam) for fibrosis detection. Paraffin-embedded liver tissues were used for H&E, TUNEL, BrdU, PAS, PAS diastase (PASD), and immunostaining, except for SMA staining. A board certified pathologist (MV) evaluated all histologic sections. Antibodies used were against: phospho-Histone H3, phospho-γH2AX, cyclin D1, cleaved caspase3, phospho-ERK (all from Cell Signaling), F4/80 (Caltag), B220 (eBioscience), and CD3 (DAKO). Sirius Red staining was performed to quantitate the amount of collagen fibers. Apoptosis was determined by the ApoAlert TUNEL Assay Kit (Clontech). To examine cell proliferation, mice were injected i.p. with 100 mg/kg BrdU (Sigma) 2 hr prior to sacrifice, and paraffin sections were stained using the BrdU in situ detection kit (BD Biosciences). To detect glycogen accumulation, PAS and PASD staining were performed. ORO, Sirius Red, SMA, F4/80, and DHE positive areas were quantified using Image J software. B220, CD3, TUNEL, cleaved-caspase3, p-γH2AX, Ki67, p-ERK, cyclin D1, BrdU, p-HH3, and cyclin B positive cells were counted in 6-10 random fields (×100, × 200 or x400) on each slide. All the quantification results are depicted in the bar graphs to the

right. All the scale bars indicate 100 μm. Remaining lobes were microdissected into tumor and nontumor tissue and stored at −80°C until analyzed.

Glucose tolerance test

For glucose tolerance test, mice were starved for 6 hrs. Blood was drawn from a tail nick at the indicated time points after i.p. injection of glucose (2 g/kg body weight), and blood glucose was instantly measured by one-touch ultra glucose meter.

Protein immunoblotting

Liver samples were homogenized in RIPA buffer and then equal amounts of liver homogenates were fractionated by SDS-PAGE and transferred onto a PVDF membrane. The membrane was incubated with antibodies to raptor, phospho-STAT3, phospho-Akt, phospho-ERK, ERK, phospho-GSK3α/β, GSK3, cyclin D1, LC3 (all from Cell signaling), phospho-p70S6K, p70S6K, cyclin B, cyclin E, cdc2, p27, STAT3 (all from Santa Cruz), tubulin (sigma), p62 (Progen), and p21 (Chemicon).

RNA isolation and RT-PCR

We extracted total RNA by TRIzol (Invitrogen). RNA (1 μg) was used to generate cDNA with iScript cDNA Synthesis Kit (Bio-Rad). Individual gene expression was quantified by SYBR Green Supermix and CFX96 Real-Time PCR system (Bio-Rad) and normalized to a housekeeping control gene, either cyclophilin or GAPDH. Primer sequences for RT-PCR are available upon request.

Determination of IL-6 and ALT level

Serum IL-6 was measured by ELISA (BD Biosciences) and ALT was detected using Infinity reagent (Thermo).

Liver triglyceride (TG) measurement

We extracted lipids from liver tissues by the Folch method. TG contents were measured with Pointe Scientifc Triglycerides Reagent.

Isolation and culturing of primary mouse hepatocytes and HCC cells

AML12 cells were maintained according to ATCC's instructions and incubated with rapamycin (Alfa Aesar) as indicated. Primary hepatocytes were isolated from 8 to 12 weeks old *Raptor*$^{F/F}$ and *Raptor*$^{\Delta hep}$ mice using collagenase perfusion as described (Leffert et al., 1979). Isolated hepatocytes were resuspended in William's E medium and plated on collagen I-coated plates in medium with serum. Cells were incubated overnight followed by protein extraction and genomic DNA analysis. DEN-induced HCC cells were isolated and cultured from a *Raptor*$^{\Delta hep}$ mouse and compared to dih10 HCC cells which were established from DEN-induced HCC in a *WT* BL6 mouse (He et al., 2010). Relative cell viability/ proliferation was determined using Cell Counting Kit-8 (Dojindo Laboratories, Japan).

Statistical Analysis

Data are presented as means ± SD or ± SEM as indicated. Differences in means were analyzed by Student's t test and one-way ANOVA. P values < 0.05 were considered significant (N.S.: $p > 0.05$,*: $p < 0.05$, **: $p < 0.01$,).

Supplementary Material

Refer to Web version on PubMed Central for supplementary material.

Acknowledgments

A.U. was supported by a Global Grant Scholarship from The Rotary Foundation; K.T. was supported by Postdoctoral Fellowship for Research Abroad, Research Fellowship for Young Scientists from the Japan Society for the Promotion of Science, and the Uehara Memorial Foundation Fellowship; J.H.L. was supported by The Elison Medical Foundation (NS-0932-12); S.S was supported by the German Research Foundation (DFG, SH721/1-1); H.N. was supported by Daiichi Sankyo Foundation for Life Science and Astellas Foundation for Research on Metabolic Disorders. M.K. is an American Cancer Society Research Professor and the Ben and Wanda Hildyard Chair for Mitochondrial and Metabolic Diseases. Research was supported by grants from the NCI, the Superfund Basic Research Program (P42ES010337 to M.K. and E.S.), The Elison Medical Foundation, and the American Association for Study of Liver Diseases/American Liver Foundation.

References

Abraham RT, Gibbons JJ. The mammalian target of rapamycin signaling pathway: twists and turns in the road to cancer therapy. Clin Cancer Res. 2007; 13:3109–3114. [PubMed: 17545512]

Barlow AD, Nicholson ML, Herbert TP. Evidence for rapamycin toxicity in pancreatic beta-cells and a review of the underlying molecular mechanisms. Diabetes. 2013; 62:2674–2682. [PubMed: 23881200]

Benjamin D, Colombi M, Moroni C, Hall MN. Rapamycin passes the torch: a new generation of mTOR inhibitors. Nat Rev Drug Discov. 2011; 10:868–880. [PubMed: 22037041]

Bentzinger CF, Romanino K, Cloetta D, Lin S, Mascarenhas JB, Oliveri F, Xia J, Casanova E, Costa CF, Brink M, et al. Skeletal muscle-specific ablation of raptor, but not of rictor, causes metabolic changes and results in muscle dystrophy. Cell Metab. 2008; 8:411–424. [PubMed: 19046572]

Bhat M, Sonenberg N, Gores GJ. The mTOR pathway in hepatic malignancies. Hepatology. 2013; 58:810–818. [PubMed: 23408390]

Buron F, Malvezzi P, Villar E, Chauvet C, Janbon B, Denis L, Brunet M, Daoud S, Cahen R, Pouteil-Noble C, et al. Profiling sirolimus-induced inflammatory syndrome: a prospective tricentric observational study. PLoS One. 2013; 8:e53078. [PubMed: 23308138]

Calle EE, Rodriguez C, Walker-Thurmond K, Thun MJ. Overweight, obesity, and mortality from cancer in a prospectively studied cohort of U.S. adults. N Engl J Med. 2003; 348:1625–1638. [PubMed: 12711737]

Castets P, Lin S, Rion N, Di Fulvio S, Romanino K, Guridi M, Frank S, Tintignac LA, Sinnreich M, Ruegg MA. Sustained activation of mTORC1 in skeletal muscle inhibits constitutive and starvation-induced autophagy and causes a severe, late-onset myopathy. Cell Metab. 2013; 17:731–744. [PubMed: 23602450]

Chiang GG, Abraham RT. Targeting the mTOR signaling network in cancer. Trends Mol Med. 2007; 13:433–442. [PubMed: 17905659]

Cornu M, Albert V, Hall MN. mTOR in aging, metabolism, and cancer. Curr Opin Genet Dev. 2013; 23:53–62. [PubMed: 23317514]

Duvel K, Yecies JL, Menon S, Raman P, Lipovsky AI, Souza AL, Triantafellow E, Ma Q, Gorski R, Cleaver S, et al. Activation of a metabolic gene regulatory network downstream of mTOR complex 1. Mol Cell. 2010; 39:171–183. [PubMed: 20670887]

Espeillac C, Mitchell C, Celton-Morizur S, Chauvin C, Koka V, Gillet C, Albrecht JH, Desdouets C, Pende M. S6 kinase 1 is required for rapamycin-sensitive liver proliferation after mouse hepatectomy. J Clin Invest. 2011; 121:2821–2832. [PubMed: 21633171]

Faloppi L, Scartozzi M, Maccaroni E, Di Pietro Paolo M, Berardi R, Del Prete M, Cascinu S. Evolving strategies for the treatment of hepatocellular carcinoma: from clinical-guided to molecularly-tailored therapeutic options. Cancer Treat Rev. 2011; 37:169–177. [PubMed: 20800360]

Galluzzi L, Morselli E, Kepp O, Vitale I, Younes AB, Maiuri MC, Kroemer G. Evaluation of rapamycin-induced cell death. Methods Mol Biol. 2012; 821:125–169. [PubMed: 22125064]

Guertin DA, Sabatini DM. Defining the role of mTOR in cancer. Cancer Cell. 2007; 12:9–22. [PubMed: 17613433]

Gwinn DM, Asara JM, Shaw RJ. Raptor is phosphorylated by cdc2 during mitosis. PLoS One. 2010; 5:e9197. [PubMed: 20169205]

Harrison DE, Strong R, Sharp ZD, Nelson JF, Astle CM, Flurkey K, Nadon NL, Wilkinson JE, Frenkel K, Carter CS, et al. Rapamycin fed late in life extends lifespan in genetically heterogeneous mice. Nature. 2009; 460:392–395. [PubMed: 19587680]

He G, Dhar D, Nakagawa H, Font-Burgada J, Ogata H, Jiang Y, Shalapour S, Seki E, Yost SE, Jepsen K, et al. Identification of liver cancer progenitors whose malignant progression depends on autocrine IL-6 signaling. Cell. 2013; 155:384–396. [PubMed: 24120137]

He G, Yu GY, Temkin V, Ogata H, Kuntzen C, Sakurai T, Sieghart W, Peck-Radosavljevic M, Leffert HL, Karin M. Hepatocyte IKKbeta/NF-kappaB inhibits tumor promotion and progression by preventing oxidative stress-driven STAT3 activation. Cancer Cell. 2010; 17:286–297. [PubMed: 20227042]

Health., U. N. I. o.. Global Study Looking at the Combination of RAD001 Plus Best Supportive Care (BSC) and Placebo Plus BSC to Treat Patients With Advanced Hepatocellular Carcinoma (EVOLVE-1). 2013. Available at http://clinicaltrials.gov/ct2/show/NCT01035229?term=EVOLVE-1&rank=1

Heitman J, Movva NR, Hall MN. Targets for cell cycle arrest by the immunosuppressant rapamycin in yeast. Science. 1991; 253:905–909. [PubMed: 1715094]

Hu TH, Huang CC, Lin PR, Chang HW, Ger LP, Lin YW, Changchien CS, Lee CM, Tai MH. Expression and prognostic role of tumor suppressor gene PTEN/MMAC1/TEP1 in hepatocellular carcinoma. Cancer. 2003; 97:1929–1940. [PubMed: 12673720]

Johnson SC, Rabinovitch PS, Kaeberlein M. mTOR is a key modulator of ageing and age-related disease. Nature. 2013; 493:338–345. [PubMed: 23325216]

Lamming DW, Ye L, Katajisto P, Goncalves MD, Saitoh M, Stevens DM, Davis JG, Salmon AB, Richardson A, Ahima RS, et al. Rapamycin-induced insulin resistance is mediated by mTORC2 loss and uncoupled from longevity. Science. 2012; 335:1638–1643. [PubMed: 22461615]

Leffert HL, Koch KS, Moran T, Williams M. Liver cells. Methods Enzymol. 1979; 58:536–544. [PubMed: 423789]

LoPiccolo J, Blumenthal GM, Bernstein WB, Dennis PA. Targeting the PI3K/Akt/mTOR pathway: effective combinations and clinical considerations. Drug Resist Updat. 2008; 11:32–50. [PubMed: 18166498]

Maeda S, Kamata H, Luo JL, Leffert H, Karin M. IKKbeta couples hepatocyte death to cytokine-driven compensatory proliferation that promotes chemical hepatocarcinogenesis. Cell. 2005; 121:977–990. [PubMed: 15989949]

Massoud O, Wiesner RH. The use of sirolimus should be restricted in liver transplantation. J Hepatol. 2012; 56:288–290. [PubMed: 21741926]

Matter MS, Decaens T, Andersen JB, Thorgeirsson SS. Targeting the mTOR pathway in hepatocellular carcinoma: Current state and future trends. J Hepatol. 2013

Menon S, Manning BD. Common corruption of the mTOR signaling network in human tumors. Oncogene. 2008; 27(Suppl 2):S43–51. [PubMed: 19956179]

Menon S, Yecies JL, Zhang HH, Howell JJ, Nicholatos J, Harputlugil E, Bronson RT, Kwiatkowski DJ, Manning BD. Chronic activation of mTOR complex 1 is sufficient to cause hepatocellular carcinoma in mice. Sci Signal. 2012; 5:ra24. [PubMed: 22457330]

Mercalli A, Calavita I, Dugnani E, Citro A, Cantarelli E, Nano R, Melzi R, Maffi P, Secchi A, Sordi V, Piemonti L. Rapamycin unbalances the polarization of human macrophages to M1. Immunology. 2013; 140:179–190. [PubMed: 23710834]

Merlen G, Gentric G, Celton-Morizur S, Foretz M, Guidotti JE, Fauveau V, Leclerc J, Viollet B, Desdouets C. AMPKalpha1 controls hepatocyte proliferation independently of energy balance by regulating Cyclin A2 expression. J Hepatol. 2013

Nakashima A, Maruki Y, Imamura Y, Kondo C, Kawamata T, Kawanishi I, Takata H, Matsuura A, Lee KS, Kikkawa U, et al. The yeast Tor signaling pathway is involved in G2/M transition via polo-kinase. PLoS One. 2008; 3:e2223. [PubMed: 18493323]

Neff F, Flores-Dominguez D, Ryan DP, Horsch M, Schroder S, Adler T, Afonso LC, Aguilar-Pimentel JA, Becker L, Garrett L, et al. Rapamycin extends murine lifespan but has limited effects on aging. J Clin Invest. 2013; 123:3272–3291. [PubMed: 23863708]

Novaritis, m. r. Novartis study of Afinitor® in advanced liver cancer does not meet primary endpoint of overall survival. 2013. Available at http://www.novartis.com/newsroom/media-releases/en/2013/1721562.shtml

Park EJ, Lee JH, Yu GY, He G, Ali SR, Holzer RG, Osterreicher CH, Takahashi H, Karin M. Dietary and genetic obesity promote liver inflammation and tumorigenesis by enhancing IL-6 and TNF expression. Cell. 2010; 140:197–208. [PubMed: 20141834]

Peddi VR, Wiseman A, Chavin K, Slakey D. Review of combination therapy with mTOR inhibitors and tacrolimus minimization after transplantation. Transplant Rev (Orlando). 2013; 27:97–107. [PubMed: 23932018]

Ramirez-Valle F, Badura ML, Braunstein S, Narasimhan M, Schneider RJ. Mitotic raptor promotes mTORC1 activity, G(2)/M cell cycle progression, and internal ribosome entry site-mediated mRNA translation. Mol Cell Biol. 2010; 30:3151–3164. [PubMed: 20439490]

Sabatini DM. mTOR and cancer: insights into a complex relationship. Nat Rev Cancer. 2006; 6:729–734. [PubMed: 16915295]

Shaw RJ, Cantley LC. Ras, PI(3)K and mTOR signalling controls tumour cell growth. Nature. 2006; 441:424–430. [PubMed: 16724053]

Singh R, Kaushik S, Wang Y, Xiang Y, Novak I, Komatsu M, Tanaka K, Cuervo AM, Czaja MJ. Autophagy regulates lipid metabolism. Nature. 2009; 458:1131–1135. [PubMed: 19339967]

Vezina C, Kudelski A, Sehgal SN. Rapamycin (AY-22,989), a new antifungal antibiotic. I. Taxonomy of the producing streptomycete and isolation of the active principle. J Antibiot (Tokyo). 1975; 28:721–726. [PubMed: 1102508]

Watt KD. Reducing the load: the evolution and management of obesity and nonalcoholic steatohepatitis before liver transplantation. Liver Transpl. 2012; 18(Suppl 2):S52–58. [PubMed: 22821716]

Weichhart T, Costantino G, Poglitsch M, Rosner M, Zeyda M, Stuhlmeier KM, Kolbe T, Stulnig TM, Horl WH, Hengstschlager M, et al. The TSC-mTOR signaling pathway regulates the innate inflammatory response. Immunity. 2008; 29:565–577. [PubMed: 18848473]

Wullschleger S, Loewith R, Hall MN. TOR signaling in growth and metabolism. Cell. 2006; 124:471–484. [PubMed: 16469695]

Yamanaka K, Petrulionis M, Lin S, Gao C, Galli U, Richter S, Winkler S, Houben P, Schultze D, Hatano E, Schemmer P. Therapeutic potential and adverse events of everolimus for treatment of hepatocellular carcinoma – systematic review and meta-analysis. Cancer Med. 2013; 2:862–871. [PubMed: 24403259]

Yellen P, Saqcena M, Salloum D, Feng J, Preda A, Xu L, Rodrik-Outmezguine V, Foster DA. High-dose rapamycin induces apoptosis in human cancer cells by dissociating mTOR complex 1 and suppressing phosphorylation of 4E-BP1. Cell Cycle. 2011; 10:3948–3956. [PubMed: 22071574]

Zhu AX, Abrams TA, Miksad R, Blaszkowsky LS, Meyerhardt JA, Zheng H, Muzikansky A, Clark JW, Kwak EL, Schrag D, et al. Phase 1/2 study of everolimus in advanced hepatocellular carcinoma. Cancer. 2011; 117:5094–5102. [PubMed: 21538343]

Highlights

- mTORC1 inhibition results in STAT3 activation.
- Raptor ablation results in liver damage, inflammation and oxidative stress.
- Raptor ablation potentiates hepatocarcinogenesis in lean and obese mice.
- Prolonged mTORC1 inhibition results in adverse effects on liver physiology.

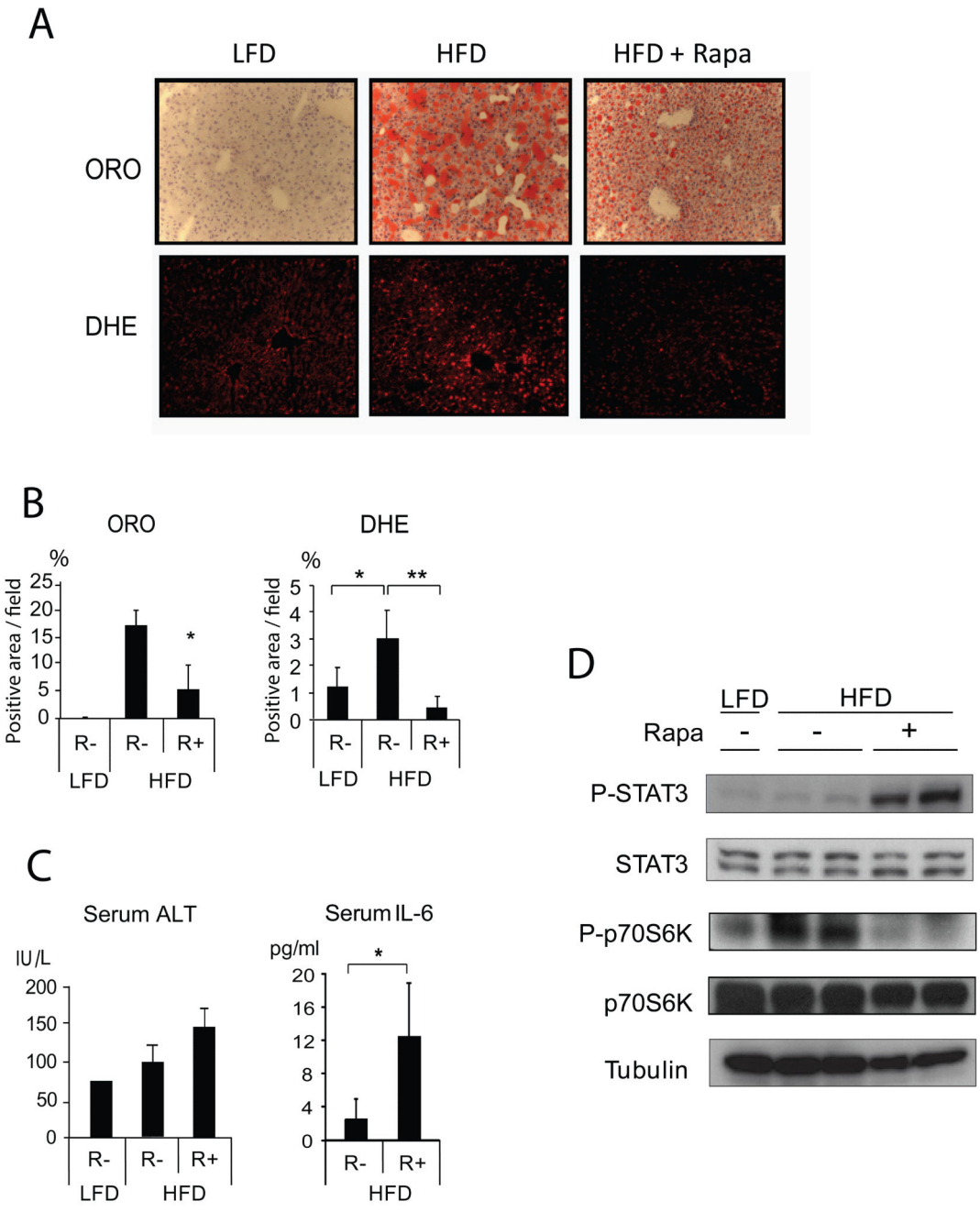

Figure 1. Rapamycin treatment enhances IL-6 expression and STAT3 activation

Eight weeks old male mice kept on normal chow (LFD) or high fat diet (HFD) for 3 months were treated with vehicle or rapamycin (5 mg/kg/d, ip) for 2 weeks. During rapamycin treatment the same feeding regimens were continued. Livers were collected and analyzed. (A) Frozen liver sections were stained for lipid droplets and ROS accumulation with oil red O (ORO) and dihydroethidium (DHE), respectively. (Magnification: 200x). (B) Data from mice in (A) were quantitated with Image J software and averaged (n=3-4). (C) Serum ALT and IL-6 were measured by Infinity reagent and ELISA, respectively (n= 3-4). (D) Livers

were homogenized and STAT3 and p70S6K expression and phosphorylation were analyzed by immunoblotting. All the bar graphs in Figure 1 represent means +/− S.D. See also Figure S1.

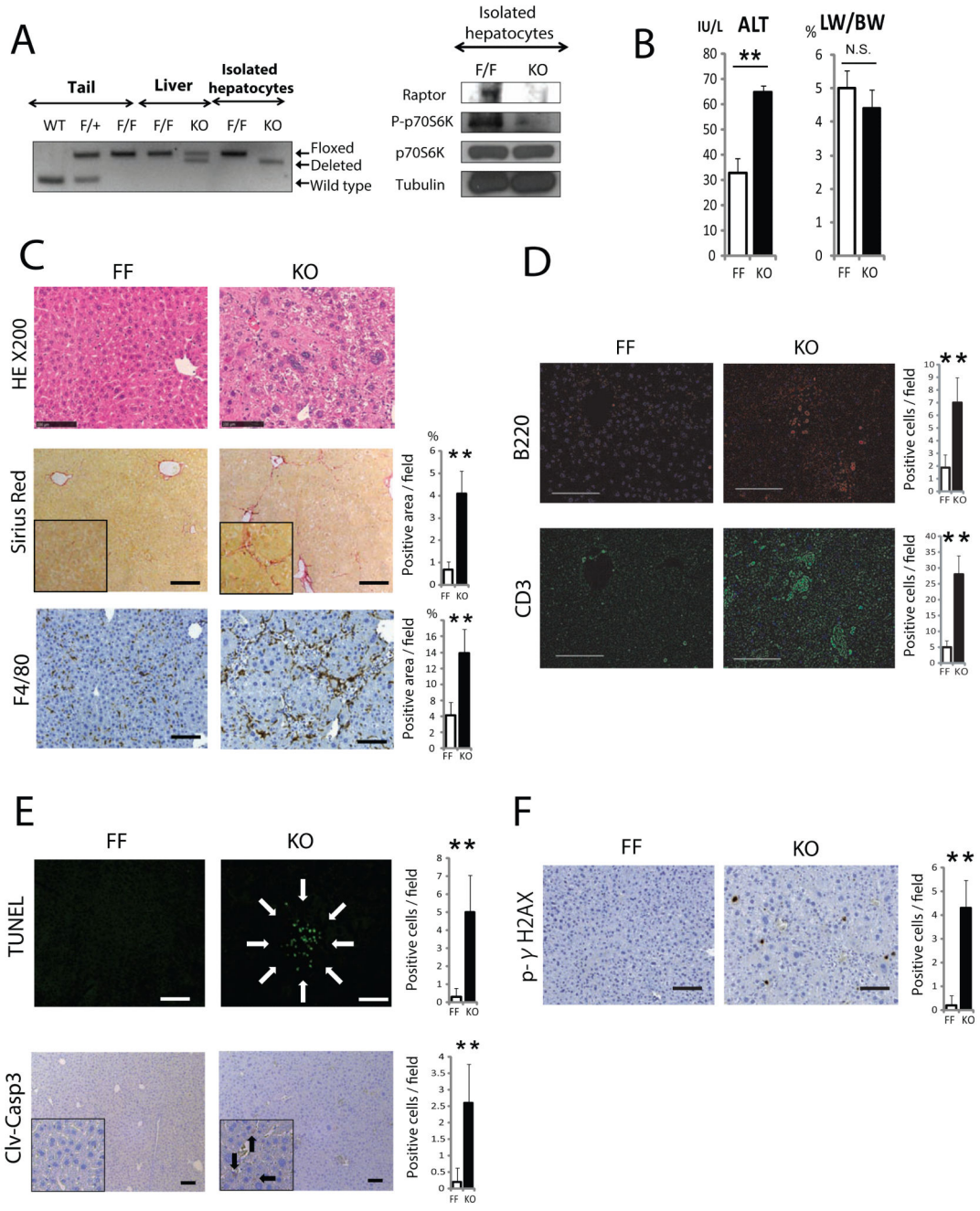

Figure 2. Characterization of liver specific Raptor knockout mice

(A) (Left panel) *Raptor* PCR on genomic DNA extracted from tail, whole liver and isolated hepatocytes of *WT*, *Raptor*$^{F/+}$ (F/+), *Raptor*$^{F/F}$ (F/F or FF), and *Raptor*$^{\Delta hep}$ (KO) mice. (Right panel) Immunoblot analysis of isolated hepatocytes from F/F and KO mice with raptor, p70S6K, and its phosphorylation antibody. (B) Serum ALT and liver weight as percentage of body weight (LW/BW) in 8 weeks old FF and KO mice (n= 4). (C, D) H&E, Sirius red, and immune cell staining of liver sections from FF and KO mice (scale bar: 100 μm). Sirius red positive areas were quantified with Image J software and shown as bar

graphs (n= 4). Immune cell infiltration was analyzed by immunostaining of liver sections with indicated antibodies. Bar graphs indicate frequencies of positive cells (n= 4). (E, F) TUNEL, cleaved-caspase 3 (clv-casp 3), and phospho-γH2AX staining were performed on liver sections, positive cells were quantified and results are shown in the bar graphs (n= 4). All the bar graphs in Figure 2 represent means +/− S.D. See also Figure S2.

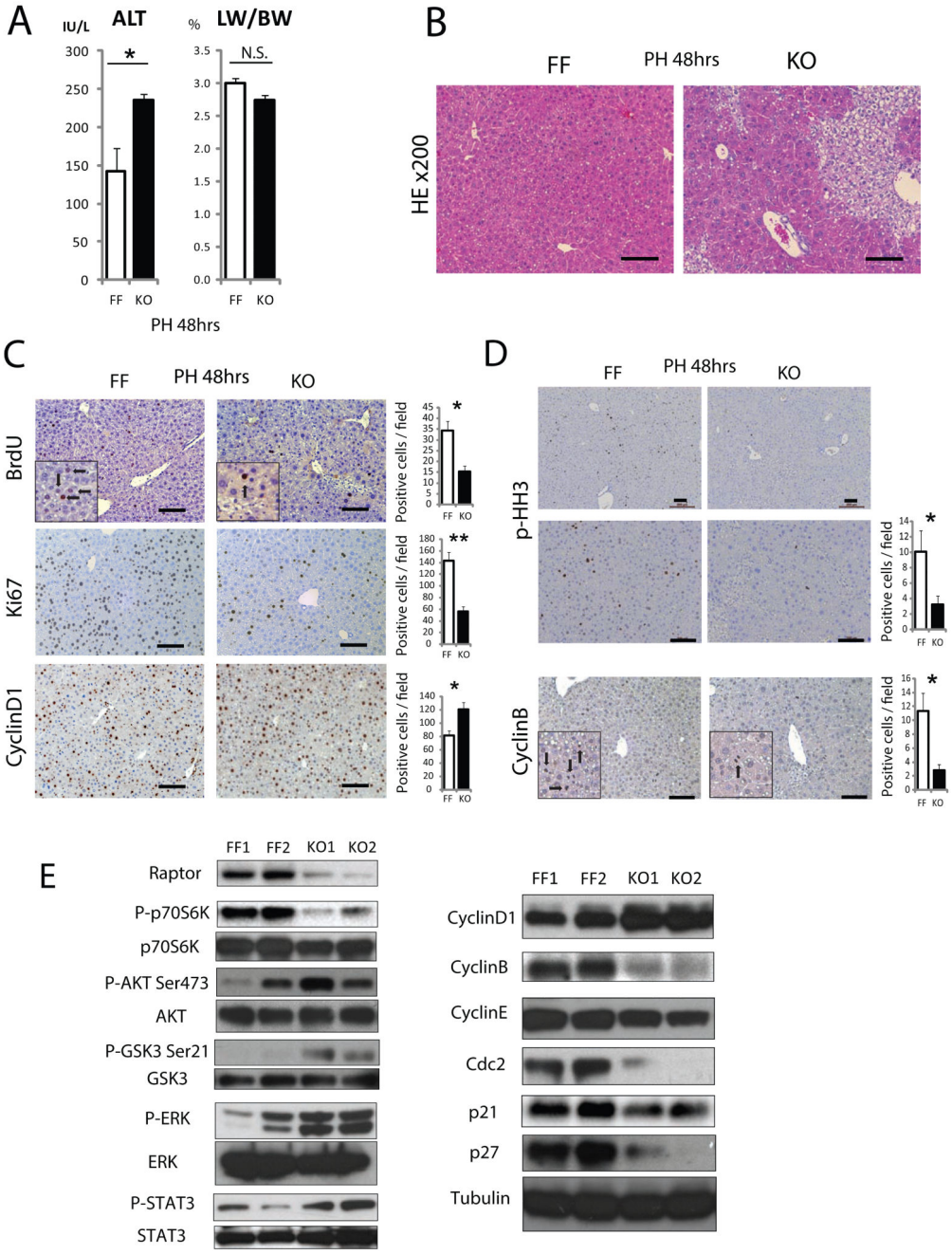

Figure 3. Loss of Raptor inhibits mitosis and results in enhanced liver damage after partial hepatectomy

(A) Serum ALT and liver weight/body weight ratio (LW/BW) in 8 weeks old *Raptor*$^{F/F}$ (FF) and *Raptor*$^{\Delta hep}$ (KO) mice 48 hrs after partial hepatectomy (PH) (n= 3). (B) Liver sections from FF and KO mice 48 hrs after PH were evaluated by H&E staining (Magnification bar: 100 μm). (C) BrdU labeling and immunostaining with antibodies to Ki67 and cyclin D1 at 48 hrs after PH. Bar graphs indicate frequencies of BrdU, Ki67, and cyclin D1 positive cells (n= 3). (D) Phospho-Histone H3 and cyclin B1 staining of liver sections from FF and KO mice after PH and their quantitative analysis (n= 3). (E) Immunoblot analysis of liver

extracts prepared 48 hrs after PH. All the bar graphs in Figure 3 represent means +/− S.D. See also Figure S3.

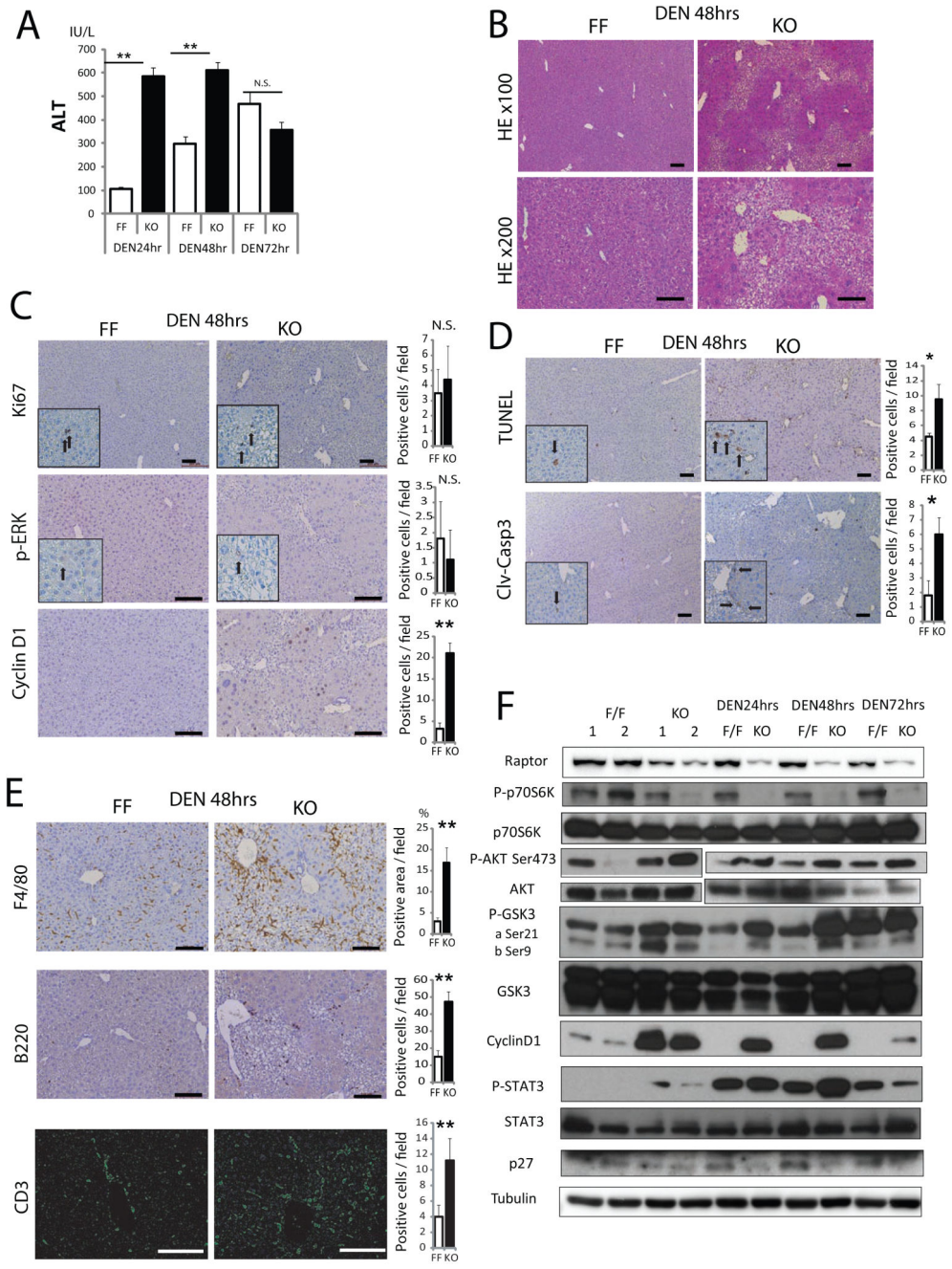

Figure 4. Loss of Raptor enhances hepatocyte death and inflammation after DEN challenge

Raptor$^{F/F}$ (FF) and *Raptor*$^{\Delta hep}$ (KO) 8 weeks old mice were i.p. injected with 100 mg/Kg DEN and their sera and livers analyzed 24-72 hrs later. (A) Serum ALT after DEN injection (n= 3). (B,C) H&E, Ki67, p-ERK, and cyclin D1 staining of liver sections from FF and KO mice 48 hrs after DEN injection (n= 3). Bar graphs indicate frequencies of Ki67, p-ERK, and cyclin D1 positive cells. (D) Cell death in FF and KO livers was analyzed 48 hrs after DEN injection by TUNEL and immunostaining with the antibody against cleaved-caspase 3 (clv-casp 3). Quantitative analysis is shown in the bar graphs (n= 3). (E) Immune cell

infiltration was analyzed 48 hrs after DEN injection by immunostaining with the indicated antibodies. F4/80 positive areas were quantified with Image J software. B220 and CD3 positive cells were counted (n= 3). (F) Immunoblot analysis of liver lysates collected after DEN injection. All the bar graphs in Figure 4 represent means +/− S.D. See also Figure S4.

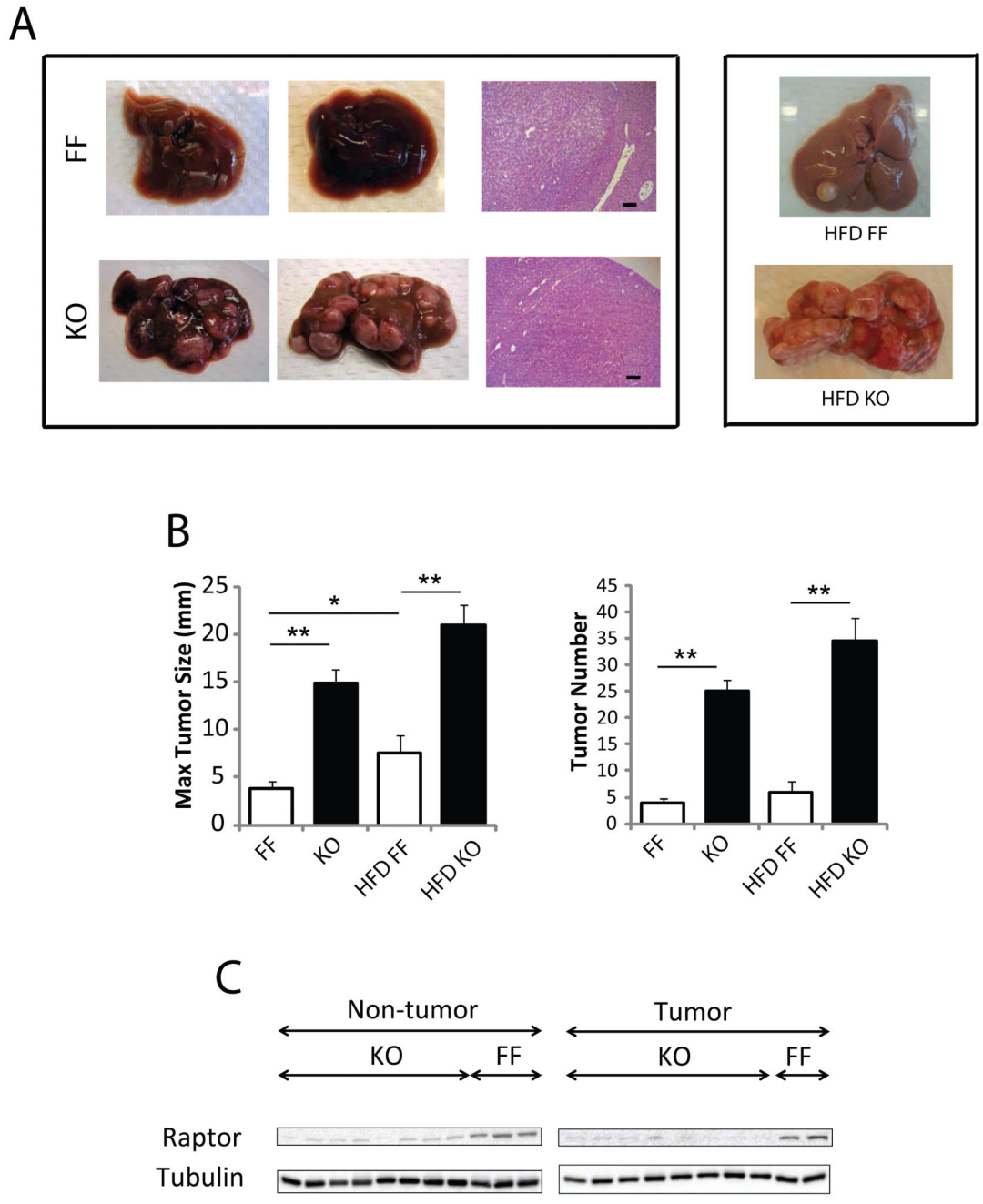

Figure 5. Increased DEN-induced hepatocarcinogenesis in *Raptor*$^{\Delta hep}$ mice

Raptor$^{F/F}$ (FF) and *Raptor*$^{\Delta hep}$ (KO) 2 weeks old males were injected with 25 mg/Kg DEN. Tumor development was analyzed 7 months later. (A) Gross morphology of livers and typical HCC histology (magnification bar; 100 μm) in mice of the indicated genotypes. (B) Tumor numbers and maximal tumor sizes. Results are means +/− S.E.M. (C) Raptor protein expression in tumor and non-tumor liver tissue was analyzed by immunoblotting. See also Figure S5.

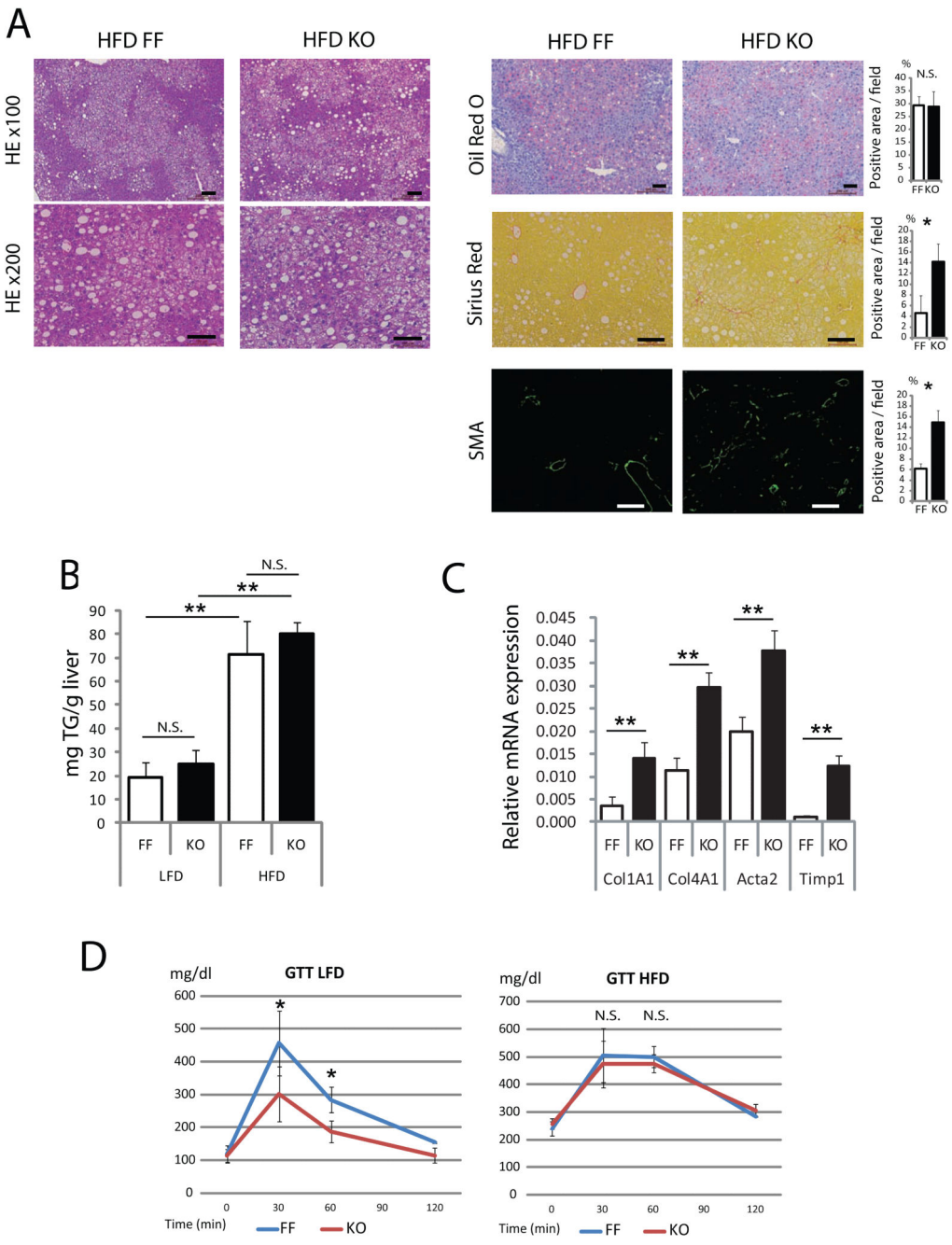

Figure 6. Hepatocyte Raptor ablation does not reduce hepatosteatosis and augments liver fibrosis in HFD fed mice

Raptor$^{F/F}$ (FF) and *Raptor*$^{\Delta hep}$ (KO) mice were kept on HFD or LFD for 6 months. (A) Liver histology, lipid accumulation and fibrosis were analyzed by staining liver sections with H&E, oil red O, Sirius Red and α smooth muscle actin (SMA) antibody. The positive areas were quantified with Image J software and shown as bar graphs. (B) Liver triglyceride (TG) content in 7 months old mice kept on LFD or HFD. (C) The mRNA amounts of fibrogenic markers, collagen α1(I) (Col1A1), collagen α1(IV) (Col4A1), actin α (Acta), and TIMP1 (Timp1) in livers of 7 months old FF and KO mice were determined by real time

qPCR. (D) Glucose tolerance tests were performed on above mice kept on LFD and HFD (n= 4). All the bar graphs in Figure 6 represent means +/− S.D. See also Figure S6.